Journal of Crystal Growth 425 (2015) 241–244

Contents lists available at ScienceDirect

Journal of Crystal Growth

journal homepage: www.elsevier.com/locate/jcrysgro

Bi flux-dependent MBE growth of GaSbBi alloys

M.K. Rajpalke [a], W.M. Linhart [a], K.M. Yu [b,c], T.S. Jones [d], M.J. Ashwin [d], T.D. Veal [a,*]

[a] Stephenson Institute for Renewable Energy and Department of Physics, School of Physical Sciences, University of Liverpool, Liverpool L69 7ZF, United Kingdom
[b] Materials Sciences Division, Lawrence Berkeley National Laboratory, 1 Cyclotron Road, Berkeley, CA 94720, USA
[c] Department of Physics and Materials Science, City University of Hong Kong, Kowloon, Hong Kong
[d] Department of Chemistry, University of Warwick, Coventry CV4 7AL, United Kingdom

ARTICLE INFO

Communicated by A. Brown
Available online 5 March 2015

Keywords:
A1. High resolution X-ray diffraction
A3. Molecular beam epitaxy
B1. Antimonides
B1. Bismuth compounds
B1. Gallium compounds
B2. Semiconducting III–V materials

ABSTRACT

The incorporation of Bi in $GaSb_{1-x}Bi_x$ alloys grown by molecular beam epitaxy is investigated as a function of Bi flux at fixed growth temperature (275 °C) and growth rate (1 μm h^{-1}). The Bi content is found to vary proportionally with Bi flux with Bi contents, as measured by Rutherford backscattering, in the range $0 < x \leq 4.5\%$. The GaSbBi samples grown at the lowest Bi fluxes have smooth surfaces free of metallic droplets. The higher Bi flux samples have surface Bi droplets. The room temperature band gap of the GaSbBi epitaxial layers determined from optical absorption decreases linearly with increasing Bi content with a reduction of ~32 meV/%Bi.

1. Introduction

The incorporation of a dilute amount of Bi in III–V arsenide semiconductors has shown great promise for optoelectronics device applications operating in the near- and mid-infrared ranges [1–5]. The interest in the incorporation of a dilute amount of N or Bi in GaSb is similarly motivated by mid-infrared applications as alloying with these elements produces a large reduction of the band gap per %N or %Bi, taking the band gap from 1.7 μm for GaSb to beyond 3 μm.

There are recent reports on controlled N incorporation and the band gap reduction in GaN_xSb_{1-x} alloys [6,7]. The incorporation of Bi as an isoelectronic dopant in GaSb was reported nearly two decades ago [8,9]. However, very few studies of the growth of $GaSb_{1-x}Bi_x$ alloys have been reported. A detailed understanding of Bi incorporation in GaSb is required in order to determine the properties of GaSbBi alloys and also to be able to develop GaNSbBi alloys lattice matched to GaSb substrates. The earliest reports on epitaxial GaSbBi alloys show very low Bi incorporation up to 0.8% [10,11]. The $GaSb_{1-x}Bi_x$ alloys grown by liquid phase epitaxy (LPE) showed the expected lattice dilation [11], whereas the initial films grown by molecular-beam epitaxy (MBE) exhibited lattice contraction with respect to GaSb [10].

The incorporation of Bi in III–V semiconductors while maintaining a droplet-free smooth surface is challenging, but is achievable by using low growth temperatures and a near-stoichiometric V:III ratio [12–14]. Some recent attempts to grow GaSbBi alloys with high Bi content show Sb/Bi droplets on the surface as well as unintentional arsenic incorporation [15]. Our first studies of growth temperature- and growth rate-dependent MBE of GaSbBi used a fixed Bi flux and achieved Bi incorporation of up to 9.6% with high substitutionality and generally metallic droplet-free surfaces [16,17]. Optical absorption, photoreflectance and photoluminescence studies showed band gap reduction of ~30–36 meV/%Bi [16,17,19,20]. However, while the Bi flux has been varied at the same time as varying the growth temperature in one previous study [10], the effect of Bi flux alone on Bi incorporation into GaSb has yet to be explored. The present work deals with the control of Bi content in GaSbBi alloys by varying the Bi flux, at fixed growth temperature and growth rate, and determination of the resulting band gap variation.

Fig. 1 shows the calculated $\mathbf{k} \cdot \mathbf{P}$ band structure close to the Γ point of GaSb and a $GaSb_{0.95}Bi_{0.05}$ alloy to illustrate the Bi-induced band gap reduction based on previous reports [16,17]. The calculation was carried out under the assumption that the valence band edge moves according to the valence band anticrossing (VBAC) model and the conduction band minimum (CBM) shifts according to the virtual crystal approximation (VCA) [16–18]. Fig. 1(a) also depicts the localised Bi 6*p*-like states at 1.17 eV below the GaSb VBM (valence band maximum) [16]. Fig. 1(b) illustrates the changes in band edge positions with respect to those of GaSb for a Bi content of 5% of the anion sublattice. According to the VBAC model, the VBM moves upward by ~10 meV/%Bi, whereas the CBM moves downward by 26.0 meV/%Bi.

* Correspondence to: Stephenson Institute for Renewable Energy and Department of Physics, School of Physical Sciences, Chadwick Building, Peach Street, University of Liverpool, Liverpool, L69 7ZF, United Kingdom. Tel.: +44 151 794 3872.
E-mail address: T.Veal@liverpool.ac.uk (T.D. Veal).

http://dx.doi.org/10.1016/j.jcrysgro.2015.02.093

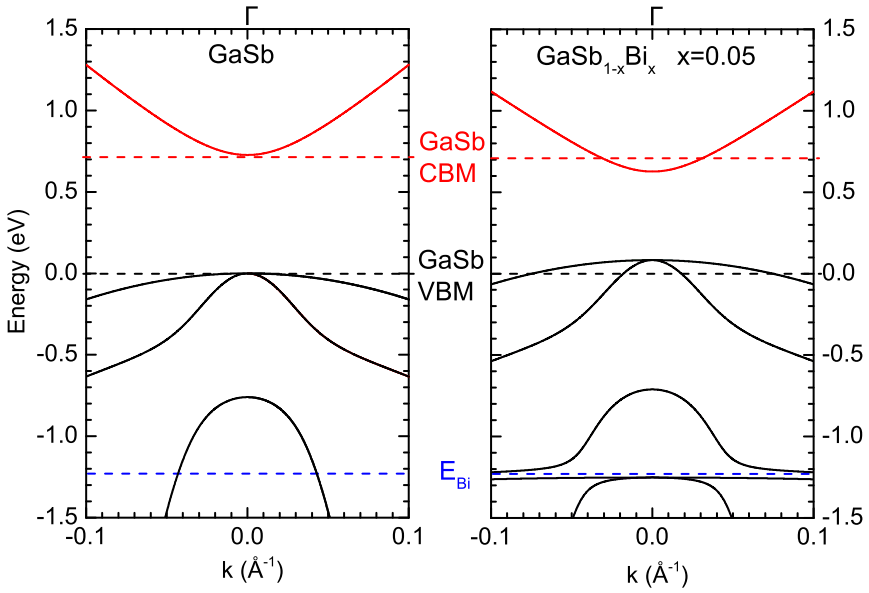

Fig. 1. (Color online) Band dispersion for (a) GaSb and (b) $GaSb_{0.95}Bi_{0.05}$ calculated using $\mathbf{k}\cdot\mathbf{p}$ model. The band gap changes from 720 to 545 meV with the incorporation of 5% Bi.

2. Experimental details

The GaSbBi epilayers were grown on undoped GaSb(001) substrates by solid-source MBE. The sources and substrate preparation procedure are described elsewhere [16]. For each GaSbBi film, a GaSb buffer layer of 100 nm thickness was grown at 500 °C and the substrate was then cooled to 275 °C. The Bi beam equivalent pressure (BEP) flux was varied from approximately 2.0×10^{-8} to 5.8×10^{-8} mbar. The Sb BEP was fixed at 1.25×10^{-6} mbar. The substrate temperature was measured by thermocouple calibrated by pyrometer measurements. The samples were grown under nominally slightly group V-rich conditions (Sb:Ga ratio of approximately 1.05:1) using a growth rate of 1.0 μm h^{-1}, at fixed growth temperatures of 275 °C. The film thicknesses were found to be 400 nm by modelling the interference fringes in 004 HRXRD ω–2θ scans and this was confirmed by RBS.

The Bi incorporation in the GaSbBi epilayers was characterised using RBS with 3.72 MeV He^{2+} ions and by HRXRD using a Philips X'Pert diffractometer equipped with a Cu Kα_1 X-ray source (λ=0.15406 nm). The surface morphology was investigated by JEOL JSM-7001F field emission scanning electron microscopy (SEM), with energy dispersive X-ray spectroscopy (EDS) used to identify any surface metallic droplets. To remove any droplets, samples were dipped in dilute HCl (10:1H_2O:HCl) for 60 s at room temperature and then rinsed in deionised water and dried in flowing nitrogen gas. Transmittance measurements were carried out at room temperature to determine the band gap of the alloys using a Bruker Vertex 70 V Fourier-transform infrared (FTIR) spectrometer, using a liquid nitrogen-cooled HgCdTe detector.

3. Results and discussion

Accurate values of Bi content in GaSbBi films cannot be obtained from XRD measurements of the lattice constant by applying Vegard's law because the lattice constant of zinc blende GaBi is experimentally unknown. Therefore, RBS was used to calculate the Bi content in the GaSbBi epilayers. Fig. 2 shows the RBS Bi content in GaSbBi epilayers as a function of Bi flux. The Bi content increases linearly with the Bi flux, at fixed growth temperature and growth rate, reaching 4.5% at the highest flux used. Channeling RBS

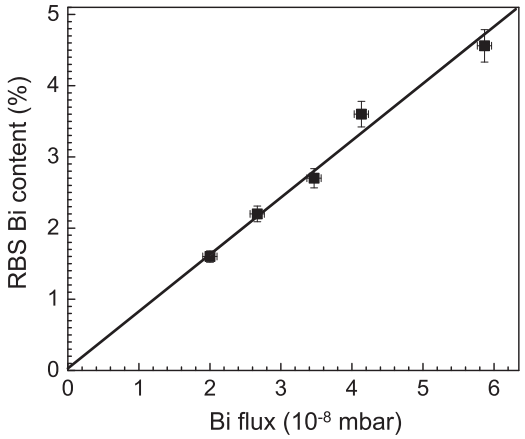

Fig. 2. (Color online) RBS Bi content of Bi flux dependent GaSbBi samples. The solid line is a linear fit to the Bi content.

measurements show that for up to 3.6% Bi content, the films are of high crystallinity with greater than 97% of Bi atoms on substitutional group V lattice sites. This falls to 93% for the sample grown using the highest Bi flux. The error bars in Fig. 2 reflect the uncertainties in the measurements of the Bi content and Bi flux. Earlier report on Bi incorporation in GaSbBi was found to saturate with higher Bi flux [10] and the maximum Bi incorporation was found to be 0.7% of the anion sublattice. The low Bi incorporation reported previously even with a high Bi flux ($\sim2.7\times10^{-7}$ mbar) is probably due to the high growth temperature (390 °C). Our earlier report showed that Bi incorporation reduces drastically at higher growth temperature ($\sim$350 °C) [16].

Fig. 3 shows the HRXRD ω–2θ scans of GaSbBi samples with Bi contents 1.6, 2.7, and 3.6%. In each case, the peak corresponding to the GaSbBi film is at a lower Bragg angle than that of the substrate. This corresponds to the expansion of the lattice of the GaSbBi epilayers with respect to the GaSb substrate. Lattice dilation has previously been observed in GaSbBi films in our previous temperature-dependent and growth rate-dependent MBE growth [16,17] and with low Bi content ($<1\%$) material grown by liquid phase epitaxy [11]. The previously observed lattice contraction for MBE-grown GaSbBi was explained in terms of group V vacancies [10]. The Pendellösung interference fringes observed indicates that the interfaces are smooth and the composition

is uniform. The diffraction peak from GaSbBi epilayers shifts towards lower angle with an increase in the Bi flux, indicating more Bi incorporation in agreement with the RBS results.

The surface morphology of the Bi flux dependent GaSbBi films was studied using SEM. Fig. 4 shows the SEM images of the GaSbBi samples with Bi contents 1.6, 2.7, 3.6, and 4.5% grown at Bi fluxes 2.0, 3.5, 4.1, and 5.8×10^{-8} mbar, respectively. Fig. 4(a) and (b) shows droplet-free smooth surfaces and are typical of GaSbBi samples with lower Bi flux ($<4.1\times10^{-8}$ mbar). At higher Bi fluxes, the films show surface Bi droplets. Fig. 4(c) and (d) shows the formation of Bi droplets, identified by EDS, on the surface of the GaSbBi films grown at higher Bi fluxes ($\geq4.1\times10^{-8}$ mbar). The excess Bi on the growth surface was etched using dilute HCl. The inset of Fig. 4(d) shows the SEM image of the same sample after HCl etching. The Bi droplets are completely removed by HCl etching.

The optical properties of the GaSbBi epilayers as a function of Bi content were studied using transmittance measurements. The absorption coefficient, α, was calculated from the transmittance data. The transmission data from each sample was divided by the transmission from a GaSb substrate so that the remaining signal corresponds to transmission through a ~400-nm thick GaSbBi layer. Fig. 5 shows the absorption spectra derived from the transmission data for the GaSbBi epilayers. The absorption edge energy red shifts with increasing Bi content. The absorption edge decreases in energy to 575 ± 20 meV as the Bi content is increased to $x=4.5\%$.

The determined band gaps are plotted in Fig. 6 along with the data points from our earlier reports on growth temperature- and

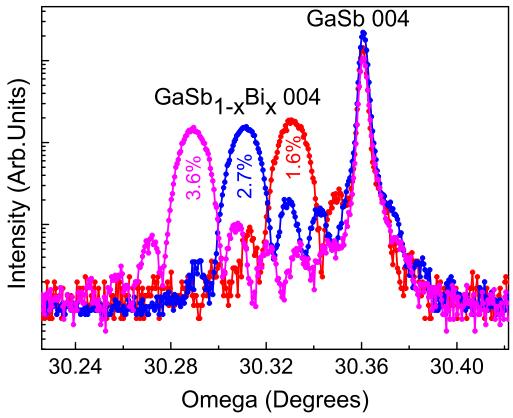

Fig. 3. (Color online) HRXRD scans of the 004 Bragg reflection of Bi flux dependent GaSbBi films on GaSb substrates with Bi content 1.6, 2.7, and 3.6% grown at 275 °C with nominal growth rate 1 μm h^{-1}.

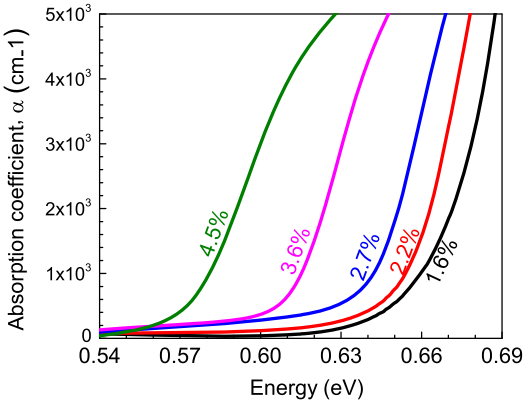

Fig. 5. (Color online) The absorption spectra for Bi flux-dependent $GaSb_{1-x}Bi_x$ films at a growth temperature of 275 °C. The composition of each film is given in the figure.

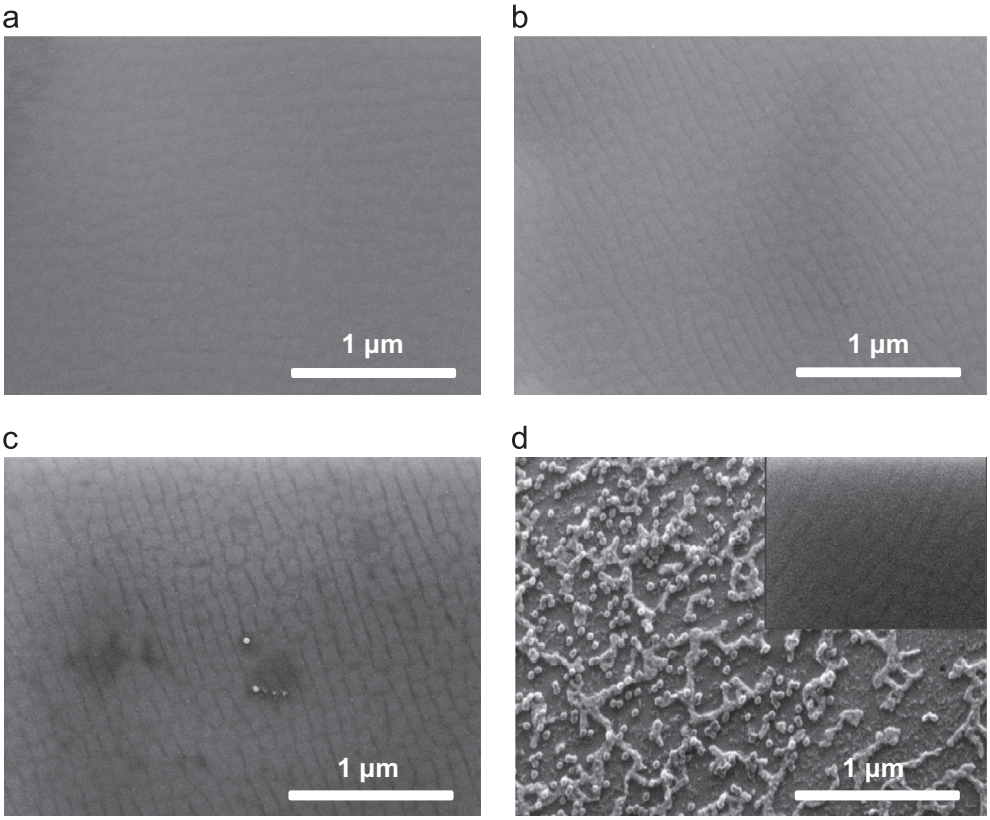

Fig. 4. (Color online) SEM images of GaSbBi samples with Bi contents (a) 1.6, (b) 2.7, (c) 3.6, and (d) 4.5% grown at Bi fluxes 2.0, 3.5, 4.1, and 5.8×10^{-8} mbar, respectively. The inset of (d) shows an SEM image of the same sample after HCl etching, indicating the removal of Bi droplets.

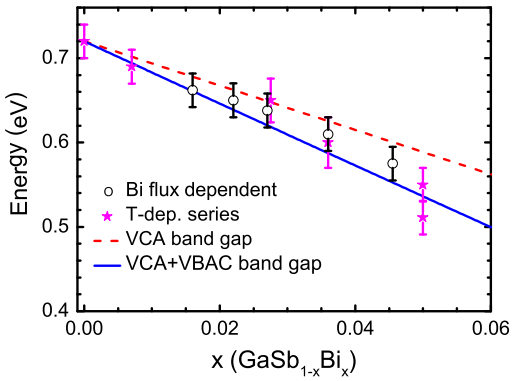

Fig. 6. (Color online) The band gap versus Bi content determined from the absorption spectra for the Bi flux-dependent GaSbBi samples (open circles). Calculated composition dependence of the band gap of $GaSb_{1-x}Bi_x$ based on the VCA variation of both the CBM and the VBM (dashed line) and from combining the VCA variation of the CBM with VBAC (solid line). The band gaps of $GaSb_{1-x}Bi_x$ films grown at different temperature (stars) from Ref. [16] are also plotted.

growth rate-dependent samples [16,17]. The band gap reduction for the Bi flux-dependent samples, obtained by a linear fit of the data points constrained to pass through 720 meV for GaSb, is found to be ~32 meV/%Bi, greater than the value from the VCA model (dashed line) of about 25 meV/%Bi [16,18]. Additional band gap reduction has previously been accounted for by the VBAC model (solid line), implemented using a 12×12 $\mathbf{k} \cdot \mathbf{p}$ Hamiltonian [18]. The band gap reduction observed for the flux dependent samples is within the range ~30–36 meV/%Bi previously reported for temperature- and growth-rate dependent samples [16,19,17,21].

4. Conclusion

Epitaxial thin films of $GaSb_{1-x}Bi_x$ with $0 < x \leq 4.5\%$ have been achieved by varying the Bi flux. The samples grown at lower Bi flux show droplet-free smooth surfaces. All the samples show high crystalline quality with greater than 97% of the incorporated Bi found to be substitutional on the group V sublattice. The Bi incorporation is found to be proportional to the Bi flux. Room temperature absorption studies show band gap reduction of 32 meV/% as the Bi content of the GaSbBi alloys is increased.

Acknowledgements

The work at Liverpool and Warwick was supported by the Engineering and Physical Sciences Research Council (EPSRC) under Grant nos. EP/G004447/2 and EP/H021388/1. RBS measurements performed at Lawrence Berkeley National Lab were supported by the Director, Office of Science, Office of Basic Energy Sciences, Materials Sciences and Engineering Division, of the U.S. Department of Energy under Contract no. DE-AC02-05CH11231.

References

[1] Y. Tominaga, Y. Kinoshita, K. Oe, M. Yoshimoto, Appl. Phys. Lett. 93 (2008) 131915.
[2] P.M. Asbeck, R.J. Welty, C.W. Tu, H.P. Xin, R.E. Welser, Semicond. Sci. Technol. 17 (2002) 898.
[3] B. Fluegel, S. Francoeur, A. Mascarenhas, S. Tixier, E.C. Young, T. Tiedje, Phys. Rev. Lett. 97 (2006) 067205.
[4] S. Francoeur, M.-J. Seong, A. Mascarenhas, S. Tixier, M. Adamcyk, T. Tiedje, Appl. Phys. Lett. 82 (2003) 3874.
[5] X. Lu, D.A. Beaton, R.B. Lewis, T. Tiedje, Y. Zhang, Appl. Phys. Lett. 95 (2009) 041903.
[6] M.J. Ashwin, D. Walker, P.A. Thomas, T.S. Jones, T.D. Veal, J. Appl. Phys. 113 (2013) 033502.
[7] J.J. Mudd, N.J. Kybert, W.M. Linhart, L. Buckle, T. Ashley, P.D.C. King, T.S. Jones, M.J. Ashwin, T.D. Veal, Appl. Phys. Lett. 103 (2013) 042110.
[8] P. Gladkov, E. Monova, J. Weber, J. Cryst. Growth 146 (1995) 319.
[9] A. Danilewsky, S. Lauer, J. Meinhardt, K. Benz, B. Kaufmann, R. Hofmann, A. Dornen, J. Electron. Mater. 25 (1996) 1082.
[10] Y. Song, W. Shumin, I.S. Roy, P. Shi, A. Hallen, J. Vac. Sci. Technol. B 30 (2012) 02B114.
[11] S.K. Das, T.D. Das, S. Dhar, M. de la Mare, A. Krier, Infrared Phys. Technol. 55 (2012) 156.
[12] X. Lu, D.A. Beaton, R.B. Lewis, T. Tiedje, M.B. Whitwick, Appl. Phys. Lett. 92 (2008) 192110.
[13] A.J. Ptak, R. France, D.A. Beaton, K. Alberi, J. Simon, A. Mascarenhas, C.-S. Jiang, J. Cryst. Growth 338 (2012) 107.
[14] G. Vardar, S.W. Paleg, M.V. Warren, M. Kang, S. Jeon, R.S. Goldman, Appl. Phys. Lett. 102 (2013) 042106.
[15] A. Duzik, J.M. Millunchick, J. Cryst. Growth 390 (2014) 5.
[16] M.K. Rajpalke, W.M. Linhart, M. Birkett, K.M. Yu, D.O. Scanlon, J. Buckeridge, T.S. Jones, M.J. Ashwin, T.D. Veal, Appl. Phys. Lett. 103 (2013) 142106.
[17] M.K. Rajpalke, W.M. Linhart, M. Birkett, K.M. Yu, J. Alaria, J. Kopaczek, R. Kudrawiec, T.S. Jones, M.J. Ashwin, T.D. Veal, J. Appl. Phys. 105 (2014) 112102.
[18] K. Alberi, J. Wu, W. Walukiewicz, K.M. Yu, O.D. Dubon, P.S. Watkins, C.X. Wang, X. Liu, Y.-J. Cho, J. Furdyna, Phys. Rev. B 75 (2007) 045203.
[19] J. Kopaczek, R. Kudrawiec, W.M. Linhart, M.K. Rajpalke, K.M. Yu, T.S. Jones, M.J. Ashwin, J. Misiewicz, T.D. Veal, Appl. Phys. Lett. 103 (2013) 261907.
[20] J. Kopaczek, R. Kudrawiec, W. Linhart, M. Rajpalke, T. Jones, M. Ashwin, T. Veal, Appl. Phys. Express 7 (2014) 111202.
[21] M.P. Polak, P. Scharoch, R. Kudrawiec, J. Kopaczek, M.J. Winiarski, W.M. Linhart, M.K. Rajpalke, K.M. Yu, T.S. Jones, M.J. Ashwin, T.D. Veal, J. Phys. D: Appl. Phys. 47 (2014) 355107.